

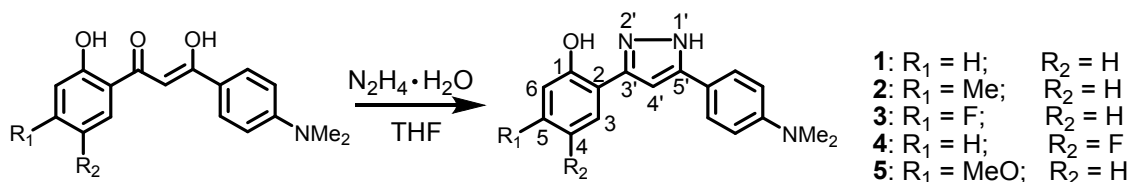
Supporting Information

**ESIPT-Active Organic Compounds with White Luminescence Based
on Crystallization-Induced Keto Emission (CIKE)**

Huapeng Liu, Xiao Cheng, Houyu Zhang, Yue Wang, Hongyu Zhang* and Shigehiro
Yamaguchi**

Table of contents

1. General information	S2–5
2. Photophysical properties	S6
3. XRD and PL spectra of compound 6	S7–8
4. Crystal structures	S9–13
5. NMR spectrum of compound 6 fumed with HOAc	S14
6. PL spectrum and PXRD of compound 7	S15
7. Calculated results of compound 1	S16–S22
8. NMR spectra	S23–30



Scheme S1. Synthetic procedure of compounds **1–5**.

Materials and Instruments. Chemicals of the highest purity level available were obtained from Acros, Sigma-Aldrich, or TCI Chemical Co., and were used without further purification. 1,3-Diaryl substituted β -diketone precursors were synthesized according to literature procedures.^{S1} NMR spectra were recorded on a Bruker Avance 500 MHz spectrometer with tetramethylsilane as the internal standard, while mass spectra were recorded on a Thermo Fisher ITQ1100 mass spectrometer. Elemental analyses were performed on a FlashEA1112 spectrometer. While UV-vis absorption spectra were recorded on a Shimadzu UV-2550 spectrophotometer, emission spectra were recorded using a Shimadzu RF-5301 PC spectrometer or a Maya2000 Pro CCD spectrometer. Absolute fluorescence quantum yields and lifetimes were measured on an Edinburgh FLS920 with or without an integrating sphere. All measurements were carried out at room temperature under ambient conditions. Melting points were determined on a Kofler hot-stage and are uncorrected.

General Synthetic Procedure. A solution of the respective 1,3-diaryl β -diketone (10 mmol) in THF (20 mL) was heated to 60 °C. After the addition of hydrazine hydrate (100 mmol), the mixture was stirred for 12 h at the same temperature. Then, solvents were removed under reduced pressure, before the resulting mixtures were recrystallized twice from CH₂Cl₂/petroleum ether (1:1, v/v) to yield the purified target compounds as white solids or colorless crystals.

5-Methyl-2-(5-[4-dimethylaminophenyl]-1*H*-pyrazole-3-yl)phenol (**2**). Yield: 90%. Mp. 216–218 °C. ¹H NMR (500 MHz, CDCl₃): δ 10.87 (s, 1H), 10.06 (s, 1H), 7.51 (d, *J* = 8.0 Hz, 1H), 7.47 (d, *J* = 9.0 Hz, 2H), 6.85 (s, 1H), 6.76 (m, 4H), 3.02 (s, 6H), 2.34 (s, 3H). ¹³C NMR (125 MHz, DMSO-*d*₆): δ 155.3, 150.3, 144.7, 138.3, 126.5, 126.4, 120.1, 117.1, 116.8, 114.4, 112.2, 97.4, 39.8, 20.9. MS m/z: 293.00 [M]⁺ (calcd: 293.15). Anal. Calcd (%) for C₁₈H₁₉N₃O: C, 73.69; H, 6.53; N, 14.32. Found: C, 73.52; H, 6.56; N, 14.40.

5-Fluoro-2-(5-[4-dimethylaminophenyl]-1*H*-pyrazole-3-yl)phenol (**3**). Yield: 93%. Mp.

226–227 °C. ^1H NMR (500 MHz, CDCl_3): δ 11.25 (s, 1H), 10.05 (s, 1H), 7.56 (dd, $J = 6.5$ Hz, 8.5 Hz, 1H), 7.47 (d, $J = 8.5$ Hz, 2H), 6.78 (d, $J = 9.0$ Hz, 2H), 6.74 (dd, $J = 2.5$ Hz, 10.5 Hz, 1H), 6.70 (s, 1H), 6.65 (td, $J = 2.5$ Hz, 8.5 Hz, 1H), 3.03 (s, 6H). ^{13}C NMR (125 MHz, $\text{DMSO}-d_6$): δ 163.1, 161.1, 156.9, 150.3, 144.05, 128.0, 126.3, 116.2, 114.1, 112.2, 106.1, 103.3, 97.6, 39.9. ^{19}F NMR (470 MHz, CDCl_3): δ -112.15. MS m/z: 296.95 [M] $^+$ (calcd: 297.13). Anal. Calcd (%) for $\text{C}_{17}\text{H}_{16}\text{FN}_3\text{O}$: C, 68.67; H, 5.42; N, 14.13. Found: C, 68.65; H, 5.48; N, 14.19.

4-Fluoro-2-(5-[4-dimethylaminophenyl]-1*H*-pyrazole-3-yl)phenol (**4**). Yield: 89%. Mp. 213–214 °C. ^1H NMR (500 MHz, CDCl_3): δ 10.78 (s, 1H), 10.23 (s, 1H), 7.47 (d, $J = 9.0$ Hz, 2H), 7.30 (dd, $J = 3.0$ Hz, 9.5 Hz, 1H), 6.94 (m, 2H), 6.78 (d, $J = 9.0$ Hz, 2H), 6.72 (s, 1H), 3.03 (s, 6H). ^{13}C NMR (125 MHz, $\text{DMSO}-d_6$): δ 156.5, 154.6, 151.5, 150.4, 144.3, 126.3, 118.0, 117.4, 116.3, 115.0, 114.9, 112.5, 112.2, 98.5, 39.8. ^{19}F NMR (470 MHz, CDCl_3): δ -125.9. MS m/z: 296.95 [M] $^+$ (calcd: 297.13). Anal. Calcd (%) for $\text{C}_{17}\text{H}_{16}\text{FN}_3\text{O}$: C, 68.67; H, 5.42; N, 14.13. Found: C, 68.74; H, 5.36; N, 14.18.

5-Methoxyl-2-(5-[4-dimethylaminophenyl]-1*H*-pyrazole-3-yl)phenol (**5**). Yield: 86%. Mp. 197–200 °C. ^1H NMR (500 MHz, CDCl_3): δ 9.91 (br, 2H), 7.51 (d, $J = 8.5$ Hz, 1H), 7.47 (d, $J = 8.5$ Hz, 2H), 6.78 (d, $J = 8.5$ Hz, 2H), 6.67 (s, 1H), 6.59 (d, $J = 2.0$ Hz, 1H), 6.52 (dd, $J = 2.5$ Hz, 8.5 Hz, 1H), 3.82 (s, 3H), 3.02 (s, 6H). ^{13}C NMR (125 MHz, $\text{DMSO}-d_6$): δ 159.9, 156.8, 151.5, 150.3, 144.0, 127.6, 126.3, 116.4, 112.2, 110.3, 105.7, 101.5, 96.9, 55.0, 39.8. MS m/z: 308.89 [M] $^+$ (calcd: 309.15). Anal. Calcd (%) for $\text{C}_{18}\text{H}_{19}\text{N}_3\text{O}_2$: C, 69.88; H, 6.19; N, 13.58. Found: C, 69.72; H, 6.08; N, 13.64.

2-(5-phenyl-1*H*-pyrazole-3-yl)phenol (**6**). Yield: 81%. Mp. 151–153 °C. ^1H NMR (500 MHz, CDCl_3): δ 10.40 (br, 2H), 7.63 (dd, $J = 1.5$ Hz, 8.0 Hz, 1H), 7.60 (d, $J = 7.5$ Hz, 2H), 7.46 (t, $J = 7.5$ Hz, 2H), 7.40 (t, $J = 7.0$ Hz, 1H), 7.24 (m, 1H), 7.06 (d, $J = 8.0$ Hz, 1H), 6.95 (t, $J = 7.5$ Hz, 1H), 6.90 (s, 1H). ^{13}C NMR (125 MHz, $\text{DMSO}-d_6$): δ 155.1, 149.78, 144.5, 130.3, 129.0, 128.2, 127.1, 125.4, 119.4, 116.9, 116.5, 100.2. MS m/z: 235.94 [M] $^+$ (calcd: 236.09). Anal. Calcd (%) for $\text{C}_{15}\text{H}_{12}\text{N}_2\text{O}$: C, 76.25; H, 5.12; N, 11.86. Found: C, 76.39; H, 5.15; N, 11.81.

3-(2-methoxyphenyl)-5-(4-dimethylaminophenyl)-1*H*-pyrazole (**7**). Yield: 73%. Mp. 88–90 °C. ^1H NMR (500 MHz, CDCl_3): δ 8.64 (br, 1H), 7.75 (m, 3H), 7.31 (m, 1H), 7.06 (t, $J = 7.5$

Hz, 2H), 7.40 (t, J = 7.0 Hz, 1H), 7.24 (m, 1H), 7.06 (d, J = 7.5 Hz, 1H), 7.02 (d, J = 8.5 Hz, 1H), 6.86 (s, 1H). 6.83 (d, J = 8.5 Hz, 2H), 3.99 (s, 3H), 3.00 (s, 6H). ^{13}C NMR (125 MHz, CDCl_3): δ 156.0, 151.3, 150.2, 142.2, 129.1, 128.0, 126.6, 121.8, 121.3, 118.3, 112.5, 111.6, 99.3, 55.7, 40.6. MS m/z: 293.46 [M]⁺ (calcd: 293.15). Anal. Calcd (%) for $\text{C}_{18}\text{H}_{19}\text{N}_3\text{O}$: C, 73.69; H, 6.53; N, 14.32. Found: C, 73.92; H, 6.49; N, 14.22.

Single-crystal X-ray Diffraction. Single-crystal X-ray diffraction data were collected on a Rigaku RAXIS-PRID diffractometer in ω -scan mode using graphite-monochromated Mo-K α radiation. Structures were solved with direct methods using the SHELXTL program and refined with full-matrix least squares on F^2 . Non-hydrogen atoms were refined anisotropically, while the positions of hydrogen atoms were calculated and refined isotropically. The structures were deposited at the CCDC under the following numbers: 1416487 (**1**), 1416488 (**2**), 1416583 (**3**), 1416489 (**5**), 1416490 (**1**·HOAc) and 1554802 (**6**).

Computational details: *Ab initio* calculations were carried out using the Gaussian 09 program.^{S2} The geometry of the ground state was optimized by density functional theory (DFT) with the CAM-B3LYP functional and the 6–31G(*d,p*) basis set. The geometry of the locally excited state (LE) and the excited state intramolecular proton transfer (ESIPT) state was optimized using TD-DFT methods with the same functional and basis set. Absorptions and emissions were simulated by TD-DFT calculations using the optimized geometries of the ground and excited states. Vertical excitations were carried out by iteratively solving 20 states. Solvent effects for CH_2Cl_2 were taken into account by using the polarizable continuum model (PCM).^{S3}

Reference

- S1 C. Kormann, I. Pimenta, S. Löber, C. Wimmer, H. Lanig, T. Clark, W. Hillen, P. Gmeiner, *ChemBioChem* **2009**, *10*, 2924.
- S2 Gaussian 09, Revision D.01, M. J. Frisch, G. W. Trucks, H. B. Schlegel, G. E. Scuseria, M. A. Robb, J. R. Cheeseman, G. Scalmani, V. Barone, B. Mennucci, G. A. Petersson, H. Nakatsuji, M. Caricato, X. Li, H. P. Hratchian, A. F. Izmaylov, J. Bloino, G. Zheng, J. L. Sonnenberg, M. Hada, M. Ehara, K. Toyota, R. Fukuda, J. Hasegawa, M. Ishida, T. Nakajima, Y. Honda, O. Kitao, H. Nakai, T. Vreven, J. A. Montgomery, Jr., J. E. Peralta, F. Ogliaro, M. Bearpark, J. J. Heyd, E. Brothers, K. N. Kudin, V. N. Staroverov, R. Kobayashi, J. Normand, K. Raghavachari, A. Rendell, J. C. Burant, S. S. Iyengar, J. Tomasi, M. Cossi, N. Rega, J. M. Millam, M. Klene, J. E. Knox, J. B. Cross, V. Bakken, C. Adamo, J. Jaramillo, R. Gomperts, R. E. Stratmann, O. Yazyev, A. J. Austin, R. Cammi, C. Pomelli, J. W. Ochterski, R. L. Martin, K. Morokuma, V. G. Zakrzewski, G. A. Voth, P. Salvador, J. J. Dannenberg, S. Dapprich, A. D. Daniels, Ö. Farkas, J. B. Foresman, J. V. Ortiz, J. Cioslowski, and D. J. Fox, Gaussian, Inc., Wallingford CT, 2009..
- S3 J. Tomasi, B. Mennucci, R. Cammi, *Chem. Rev.* **2005**, *105*, 2999.

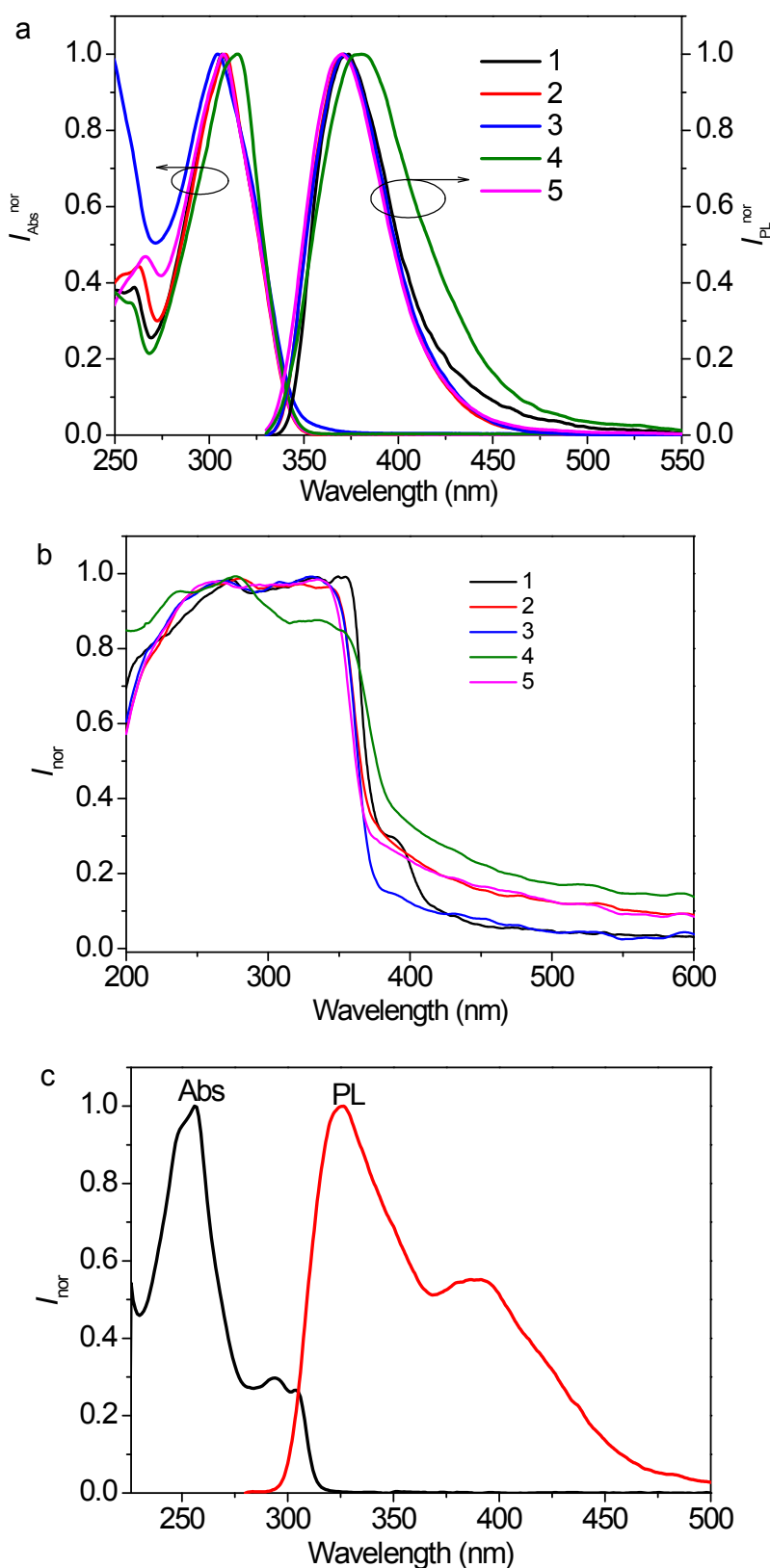


Figure S1. (a) Absorption and emission spectra of compounds **1–5** in CH_2Cl_2 (1×10^{-5} M), (b) absorption spectra of compounds **1–5** in the crystalline state and (c) absorption and emission spectra of compound **6** in CH_2Cl_2 (1×10^{-5} M).

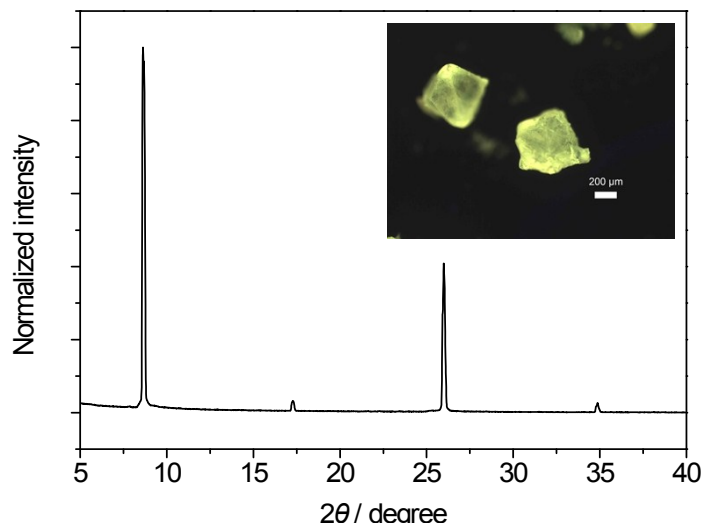


Figure S2. Powder X-ray diffraction pattern of crystalline **6** (inset is the microscopy image of **6** under UV light).

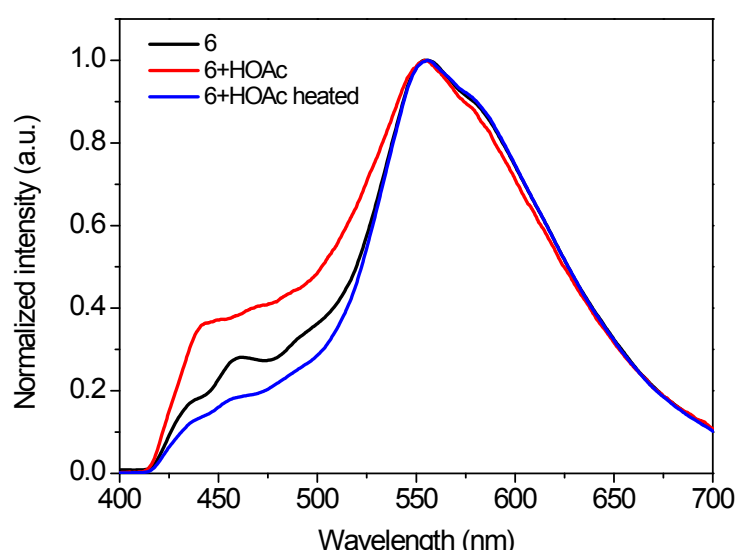


Figure S3. Emission spectra of **6** in the crystalline state, **6+HOAc** when **6** was fumed with HOAc vapor, and **6+HOAc** after heating to 80 °C for a few minutes.

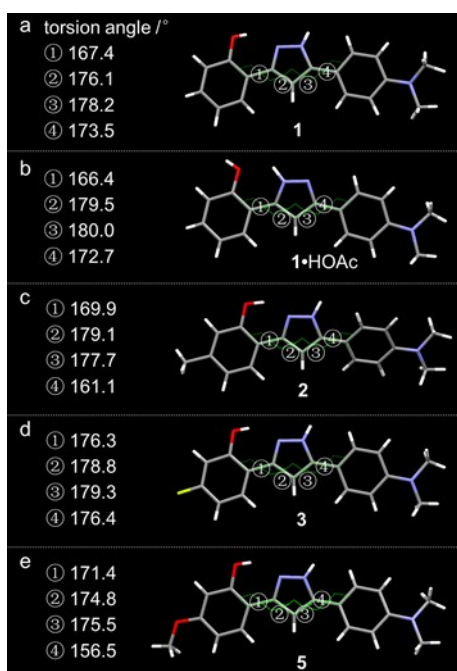


Figure S4. Molecular conformations and torsion angles of (a) **1**, (b) **1**·HOAc, (c) **2**, (d) **3**, and (e) **5** in the crystalline state.

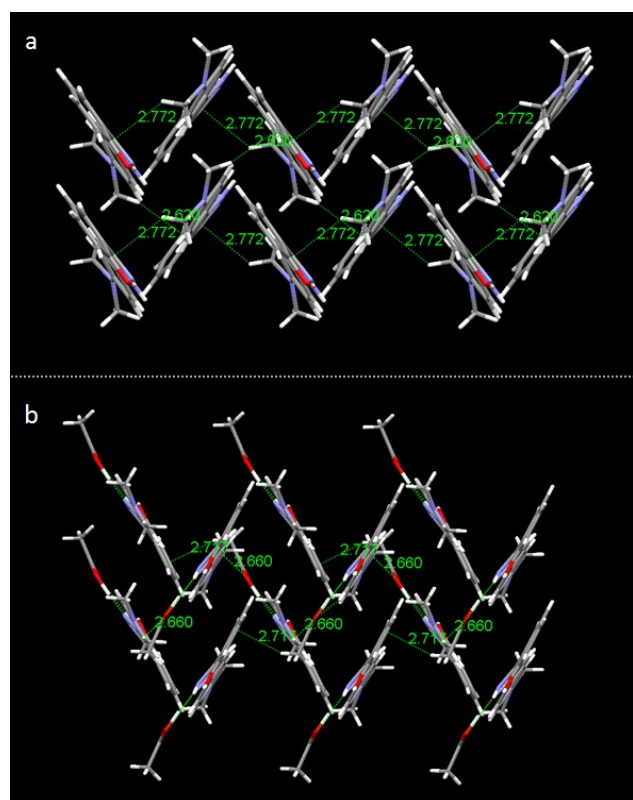


Figure S5. Intermolecular interactions in the herringbone molecular packing structure of (a) crystals **1** and (b) **1**•HOAc.

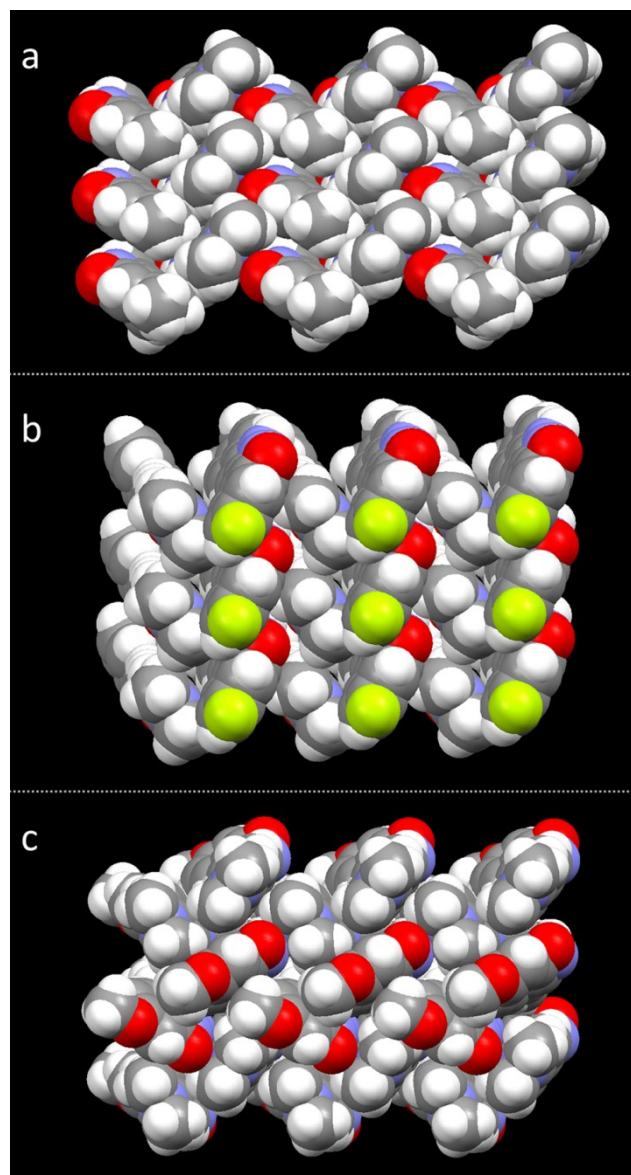


Figure S6. Crystal packing structures of (a) **2**, (b) **3**, and (c) **5**.

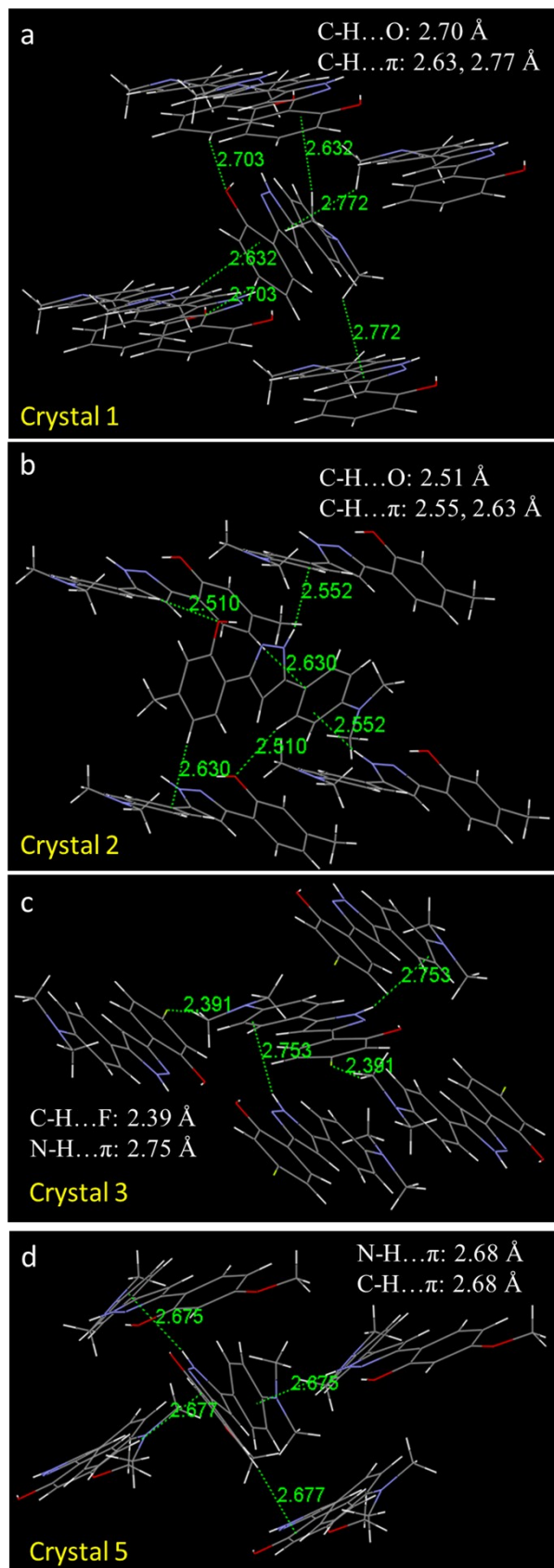


Figure S7. The type and intensity of intermolecular interactions between one molecule and its neighboring molecules in crystal (a) **1**, (b) **2**, (c) **3**, and (c) **5**.

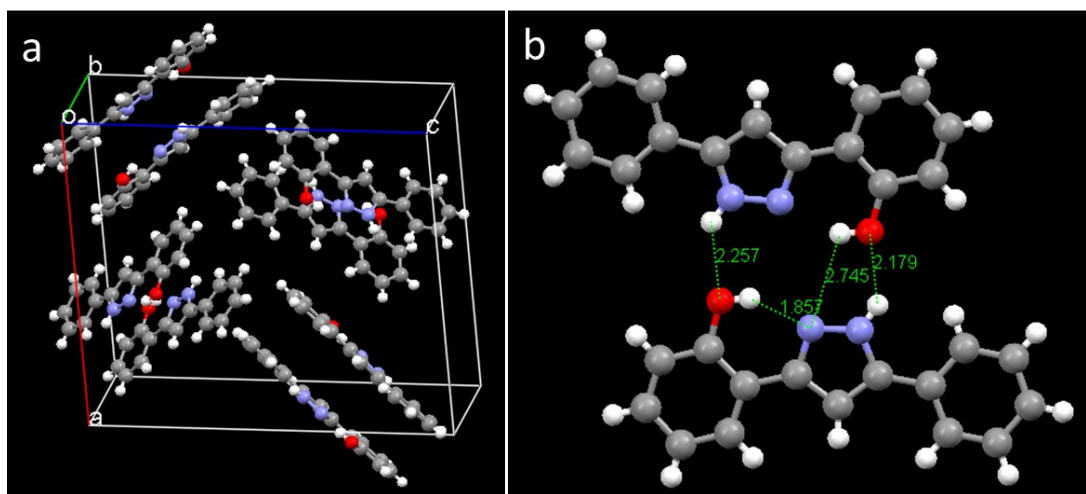


Figure S8. (a) Crystal packing structure and (b) a stable “molecule pair” structure connected by strong H-bonds in crystal **6**.

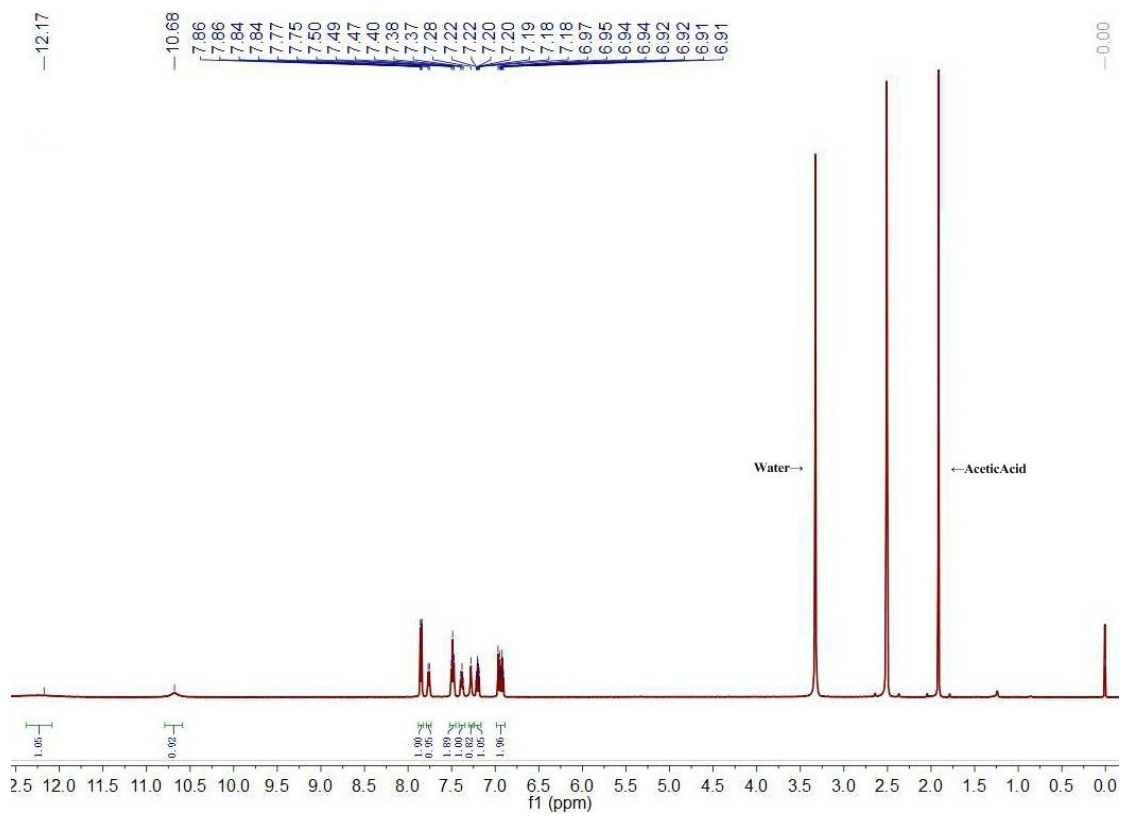


Figure S9. ¹H-NMR spectrum of compound **6** fumed with HOAC in DMSO-*d*₆ (500 MHz).

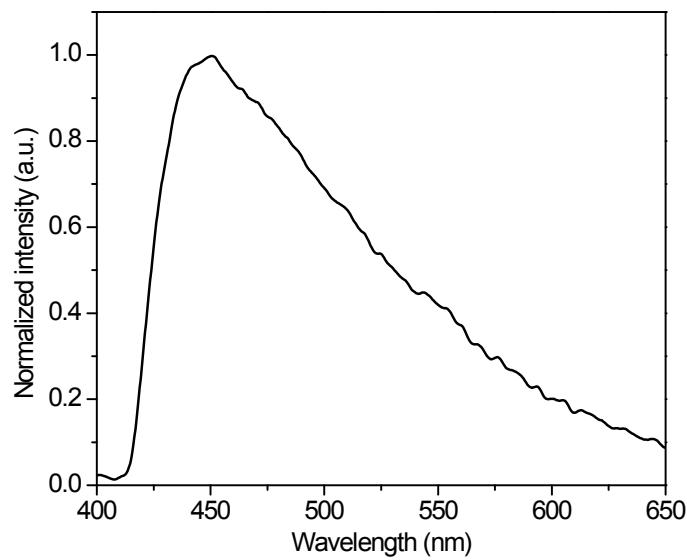


Figure S10. Emission spectrum of compound 7 in the glassy solid state.

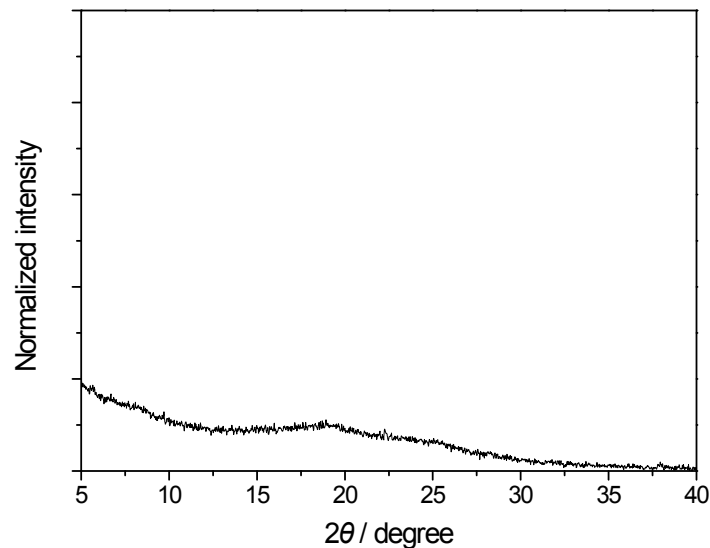


Figure S11. PXRD pattern of compound 7 in the glassy solid state.

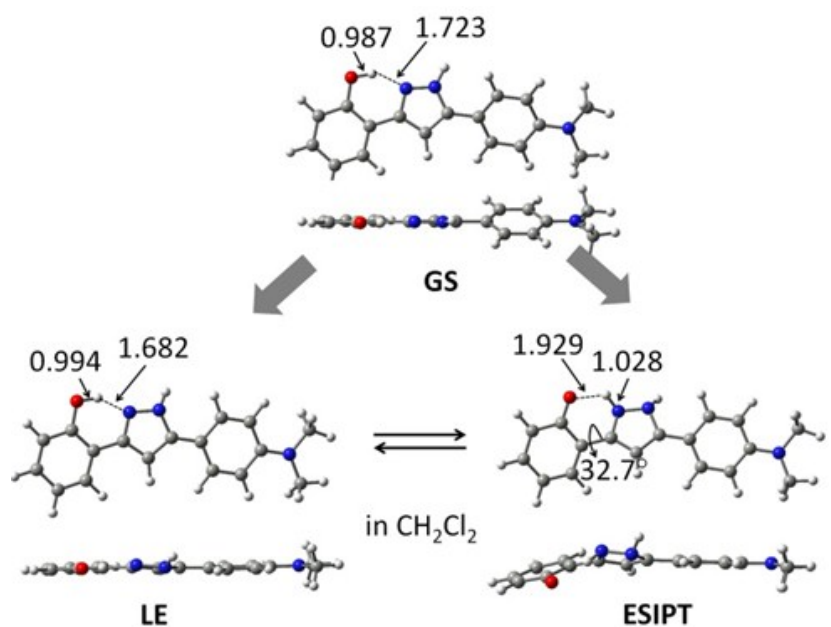


Figure S12. Molecular geometry of **1** in the ground state (GS), locally excited state (LE), and ESIPT state.

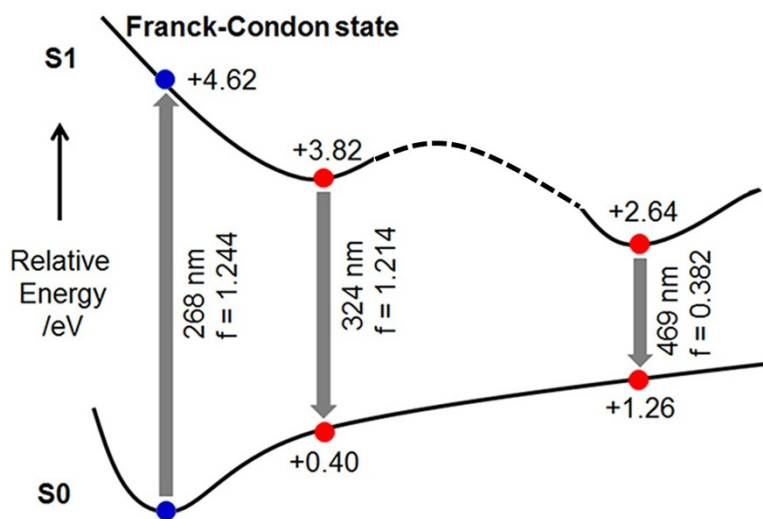


Figure S13. Schematic representation of energy diagram of the S_0 and S_1 of **1** with the relative energy levels in the GS, LE, and ESIPT states in CH_2Cl_2 , calculated at the CAM-B3LYP/6-31G(*d,p*) level of theory taking the solvent (CH_2Cl_2) into account using the PCM model.

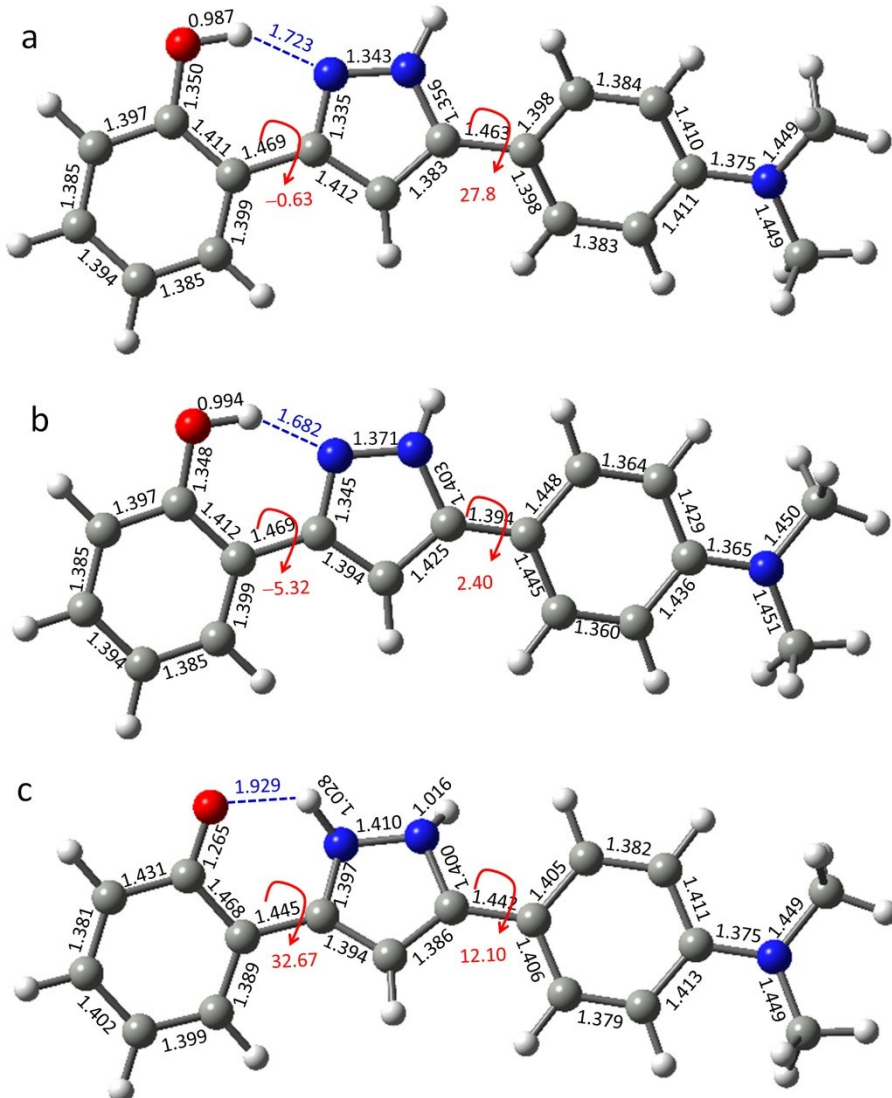


Figure S14. Bond lengths (\AA) and torsion angles ($^{\circ}$) of the optimized geometries of **1** in (a) the ground state (GS), (b) locally excited state (LE), and (c) excited-state intramolecular proton transfer state (ESIPT), calculated at the CAM-B3LYP/6-31G(*d,p*) level of theory. Solvent effects for CH_2Cl_2 were taken into account by using the polarizable continuum model (PCM) during the geometry optimization.

Table S1. TD-DFT Calculated Vertical Excitation Energies (E), Wavelengths (λ), and Oscillator Strengths (f) for Absorption and Emission of **1** in CH_2Cl_2^a

	State	Main orbital transition (CIC ^b)	E (eV)	λ (nm)	f	Exp ^c
Absorption	$S_0 \rightarrow S_1$	HOMO–1→LUMO (0.21)	4.62	268	1.244	306
		HOMO→LUMO+2 (0.17)				
		HOMO→LUMO (0.43)				
		HOMO→LUMO+1 (-0.41)				
Emission						
LE (enol form)	$S_1 \rightarrow S_0$	HOMO→LUMO (0.68)	3.82	324	1.214	374
ESIPT (keto form)	$S_1 \rightarrow S_0$	HOMO→LUMO(0.67)	2.64	469	0.382	
		HOMO→LUMO+1(0.18)				

^aTD DFT calculations were conducted at the CAM-B3LYP/6-31G(*d,p*) level of theory using the polarizable continuum model (PCM). ^bCI expansion coefficients for the main orbital transitions. ^cThe experimental values in CH_2Cl_2 .

Table S2. Cartesian Coordinates of **1** in the Ground State (GS)

N	1. 88209	-1. 47636	-0. 25499
C	-0. 06215	-0. 36325	-0. 07885
N	0. 542272	-1. 5619	-0. 26764
C	-2. 1073	1. 007549	-0. 42107
N	-5. 70567	0. 287985	-0. 0225
C	-1. 51676	-0. 20469	-0. 05394
C	-3. 47883	1. 181301	-0. 40157
C	-4. 34003	0. 130948	-0. 01959
C	-2. 36553	-1. 24138	0. 343832
O	4. 438243	-1. 96671	-0. 28133
C	-3. 74035	-1. 08681	0. 362847
C	0. 961616	0. 553991	0. 071483
C	-6. 27843	1. 596306	-0. 26931
C	5. 939044	-0. 18689	0. 014081
C	4. 622943	-0. 64548	-0. 07722
C	3. 552682	0. 265422	0. 043478
C	6. 204776	1. 156416	0. 221386
C	2. 157821	-0. 1876	-0. 04495
C	5. 157682	2. 068411	0. 341443
C	3. 851262	1. 615893	0. 252057
C	-6. 552	-0. 76447	0. 502914
H	-1. 4788	1. 832421	-0. 74153
H	-4. 35032	-1. 9176	0. 69116
H	-6. 41157	-1. 70001	-0. 04826
H	-7. 3642	1. 522121	-0. 23471
H	6. 738865	-0. 91298	-0. 08256
H	0. 848528	1. 607581	0. 270635
H	5. 359232	3. 121473	0. 503301
H	7. 233852	1. 494597	0. 289147
H	-3. 88402	2. 140526	-0. 69472
H	-1. 94871	-2. 18812	0. 674749
H	-7. 59495	-0. 47122	0. 393412
H	3. 034834	2. 324478	0. 344796
H	-6. 00333	1. 971724	-1. 26047
H	-6. 36284	-0. 96505	1. 56598
H	3. 468633	-2. 14349	-0. 32497
H	0. 101886	-2. 44436	-0. 47627
H	-5. 96254	2. 339495	0. 474774

Table S3. Cartesian Coordinates of **1** in the Locally Excited State (LE)

N	-1. 88124	-1. 49939	0. 136883
C	0. 097651	-0. 37602	-0. 01029
N	-0. 52246	-1. 63394	0. 01773
C	2. 083364	1. 106459	-0. 00751
N	5. 680091	0. 325092	0. 018335
C	1. 481196	-0. 20723	-0. 03962
C	3. 432544	1. 275051	0. 006705
C	4. 326202	0. 151262	-0. 01429
C	2. 39193	-1. 33146	-0. 09471
O	-4. 40821	-1. 9896	0. 000537
C	3. 744535	-1. 15257	-0. 07811
C	-0. 9721	0. 563864	-0. 0484
C	6. 25288	1. 65709	0. 067841
C	-5. 926	-0. 19808	-0. 0378
C	-4. 60634	-0. 65605	-0. 00472
C	-3. 54207	0. 271867	0. 021315
C	-6. 20264	1. 159179	-0. 03854
C	-2. 14562	-0. 18444	0. 037939
C	-5. 16239	2. 086924	-0. 00745
C	-3. 85261	1. 636281	0. 020984
C	6. 568073	-0. 821	-0. 01526
H	1. 439744	1. 978272	0. 016221
H	4. 384992	-2. 0238	-0. 12508
H	6. 3814	-1. 49382	0. 829695
H	7. 337213	1. 578363	0. 096101
H	-6. 72021	-0. 93649	-0. 06023
H	-0. 87875	1. 63268	-0. 15673
H	-5. 37247	3. 15086	-0. 00518
H	-7. 23425	1. 496003	-0. 06152
H	3. 83391	2. 279584	0. 034771
H	1. 99587	-2. 33641	-0. 18204
H	7. 598349	-0. 4778	0. 041957
H	-3. 04181	2. 356924	0. 048643
H	5. 924359	2. 200726	0. 961084
H	6. 446305	-1. 39549	-0. 94144
H	-3. 428	-2. 15184	0. 034401
H	-0. 12135	-2. 41728	0. 519057
H	5. 973974	2. 247245	-0. 81314

Table S4. Cartesian Coordinates of **1** in the ESIPT State

N	1. 885974	-1. 45652	-0. 70097
C	-0. 05676	-0. 37118	-0. 24449
N	0. 500024	-1. 6286	-0. 50855
C	-2. 06514	1. 087507	-0. 13135
N	-5. 67133	0. 33443	0. 108071
C	-1. 48422	-0. 19231	-0. 14535
C	-3. 42961	1. 26577	-0. 03716
C	-4. 30882	0. 161858	0. 037391
C	-2. 35817	-1. 28869	-0. 05781
O	4. 183599	-1. 87674	0. 639674
C	-3. 72717	-1. 12335	0. 032528
C	0. 983566	0. 53113	-0. 09044
C	-6. 22118	1. 665449	0. 269149
C	5. 880709	-0. 24564	0. 539487
C	4. 532736	-0. 69192	0. 36594
C	3. 547253	0. 28313	-0. 11704
C	6. 235712	1. 070322	0. 320294
C	2. 181054	-0. 14951	-0. 30424
C	5. 273963	1. 990037	-0. 12179
C	3. 954831	1. 588155	-0. 3595
C	-6. 53106	-0. 81289	0. 316702
H	-1. 43059	1. 964651	-0. 20745
H	-4. 3501	-2. 00446	0. 112098
H	-6. 41922	-1. 54525	-0. 48956
H	-7. 30749	1. 600339	0. 305704
H	6. 593954	-0. 97522	0. 907327
H	0. 892951	1. 56324	0. 21293
H	5. 55367	3. 023809	-0. 29245
H	7. 255737	1. 397186	0. 491265
H	-3. 8203	2. 274718	-0. 02898
H	-1. 95391	-2. 29551	-0. 02877
H	-7. 56921	-0. 4845	0. 322517
H	3. 237314	2. 30763	-0. 73993
H	-5. 95588	2. 311764	-0. 57412
H	-6. 32781	-1. 32271	1. 268105
H	2. 481669	-2. 14674	-0. 22619
H	0. 077874	-2. 15993	-1. 26465
H	-5. 87637	2. 152481	1. 190993

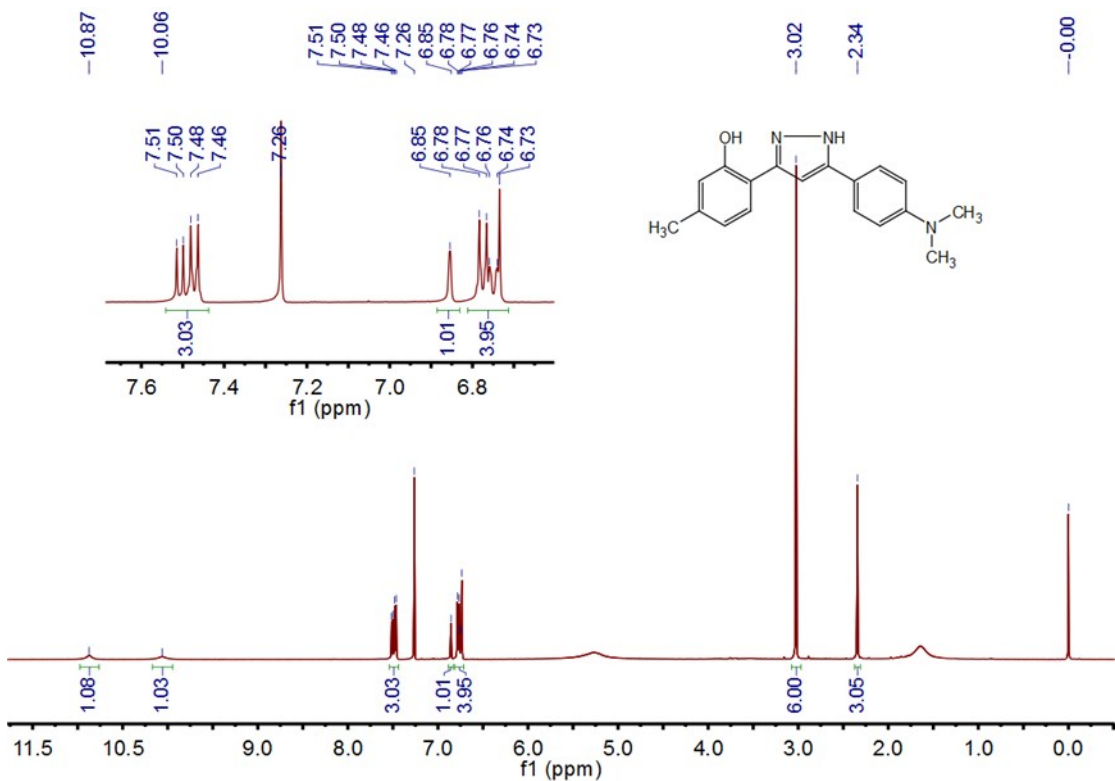


Figure S15. ¹H-NMR spectrum of compound 2 in CDCl_3 (500 MHz).

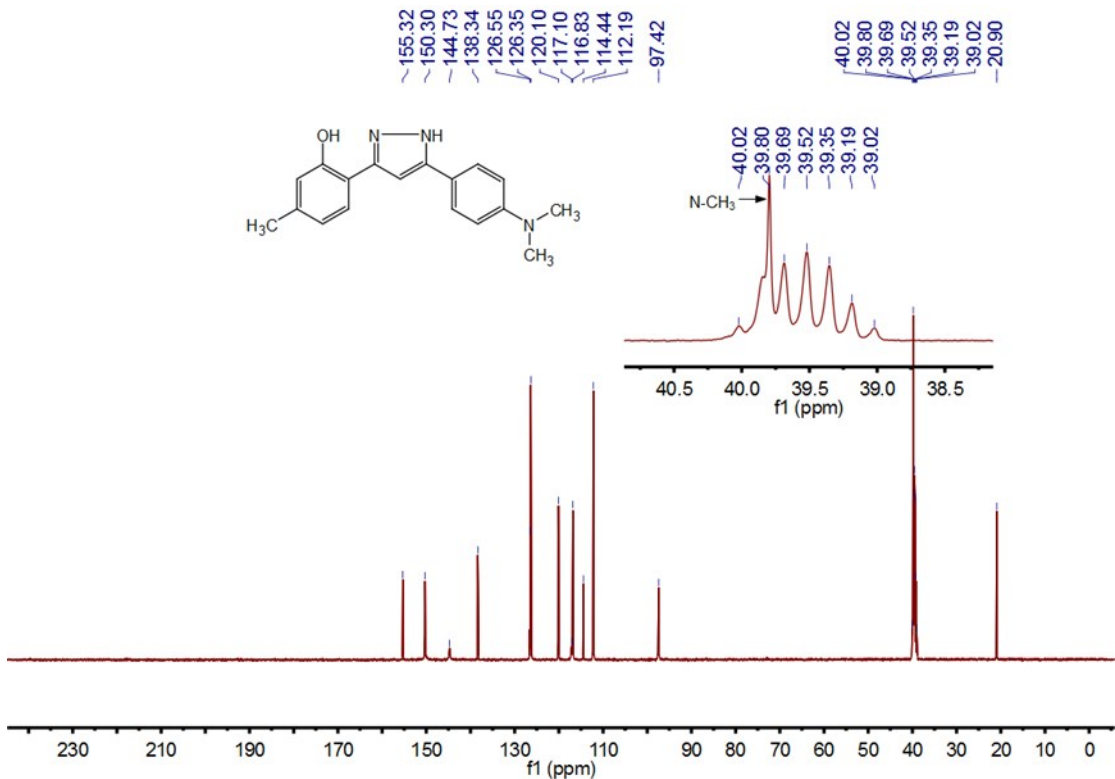


Figure S16. ¹³C-NMR spectrum of compound 2 in $\text{DMSO}-d_6$ (125 MHz).

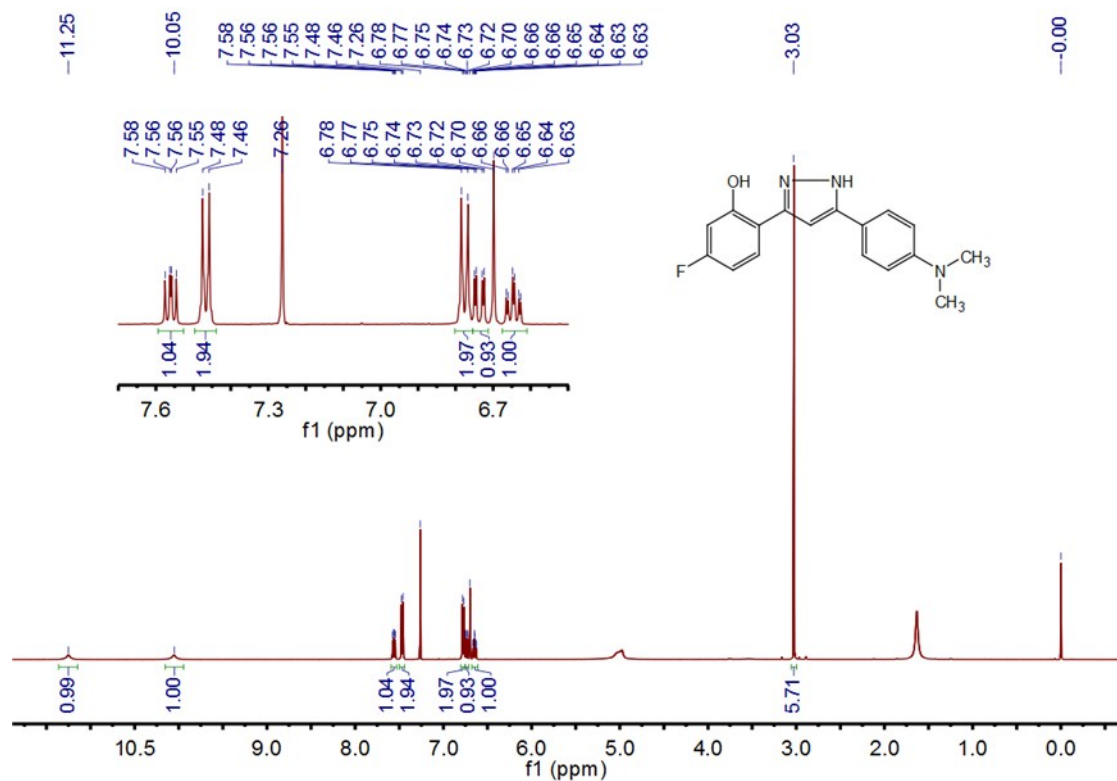


Figure S17. ^1H -NMR spectrum of compound 3 in CDCl_3 (500 MHz).

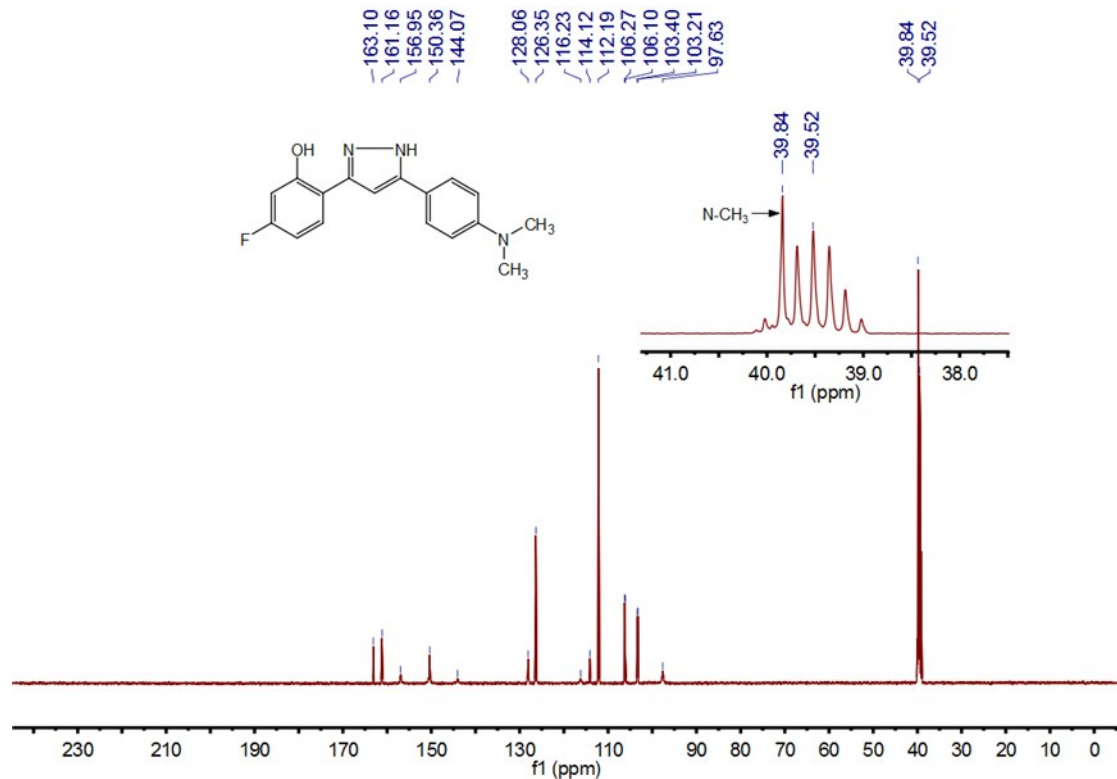


Figure S18. ^{13}C -NMR spectrum of compound 3 in $\text{DMSO}-d_6$ (125 MHz).

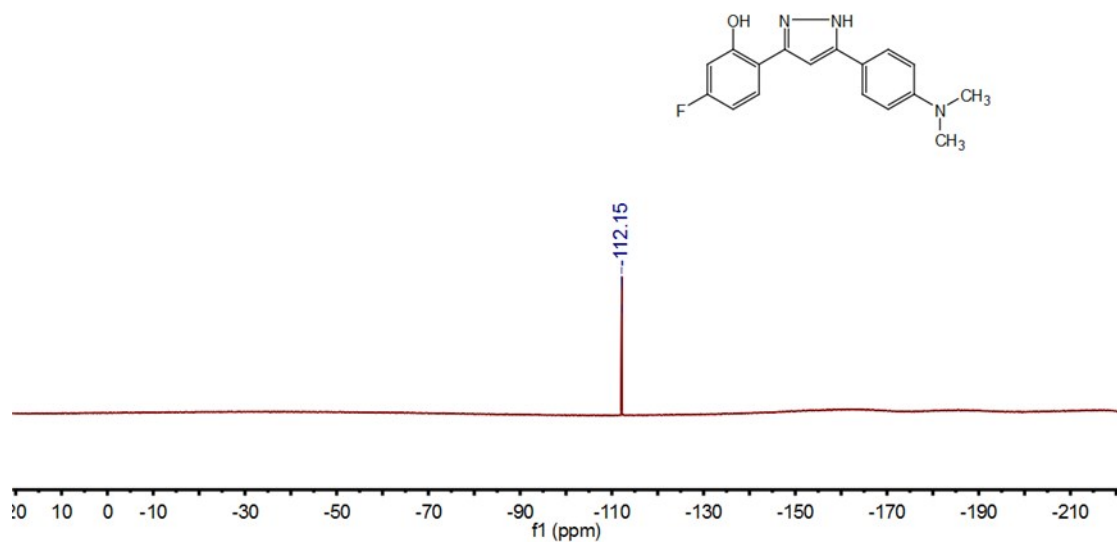


Figure S19. ^{19}F -NMR spectrum of compound 3 in CDCl_3 (470 MHz).

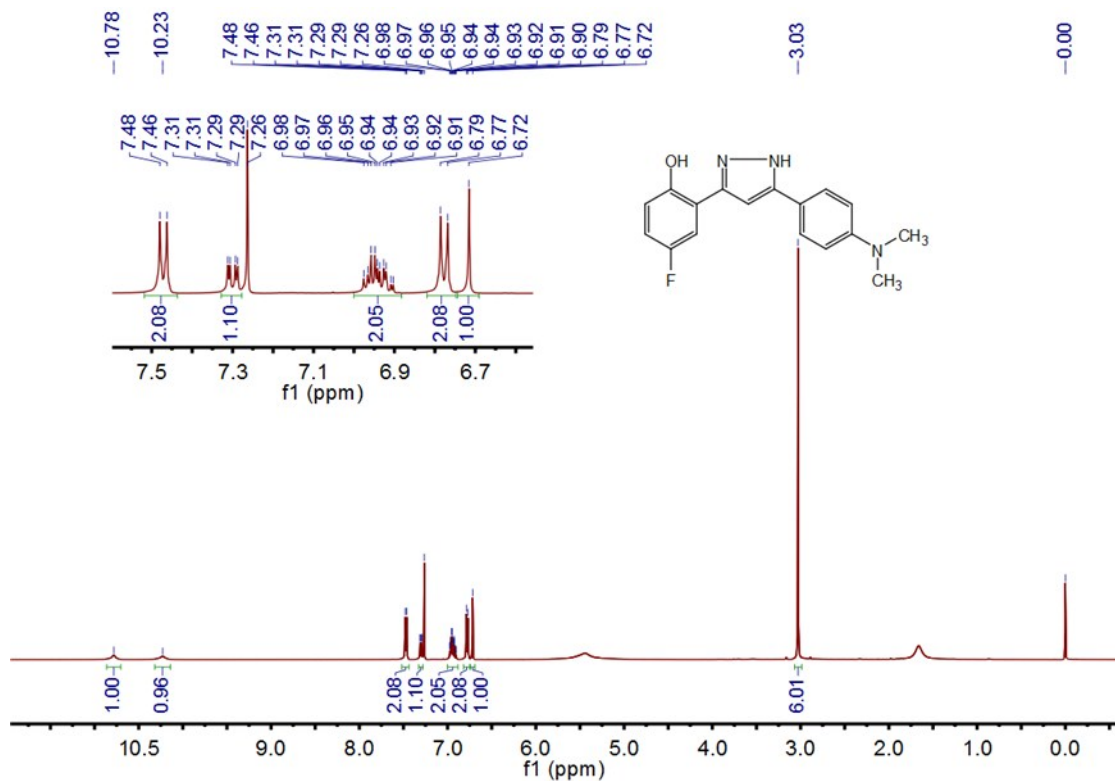


Figure S20. ^1H -NMR spectrum of compound **4** in CDCl_3 (500 MHz).

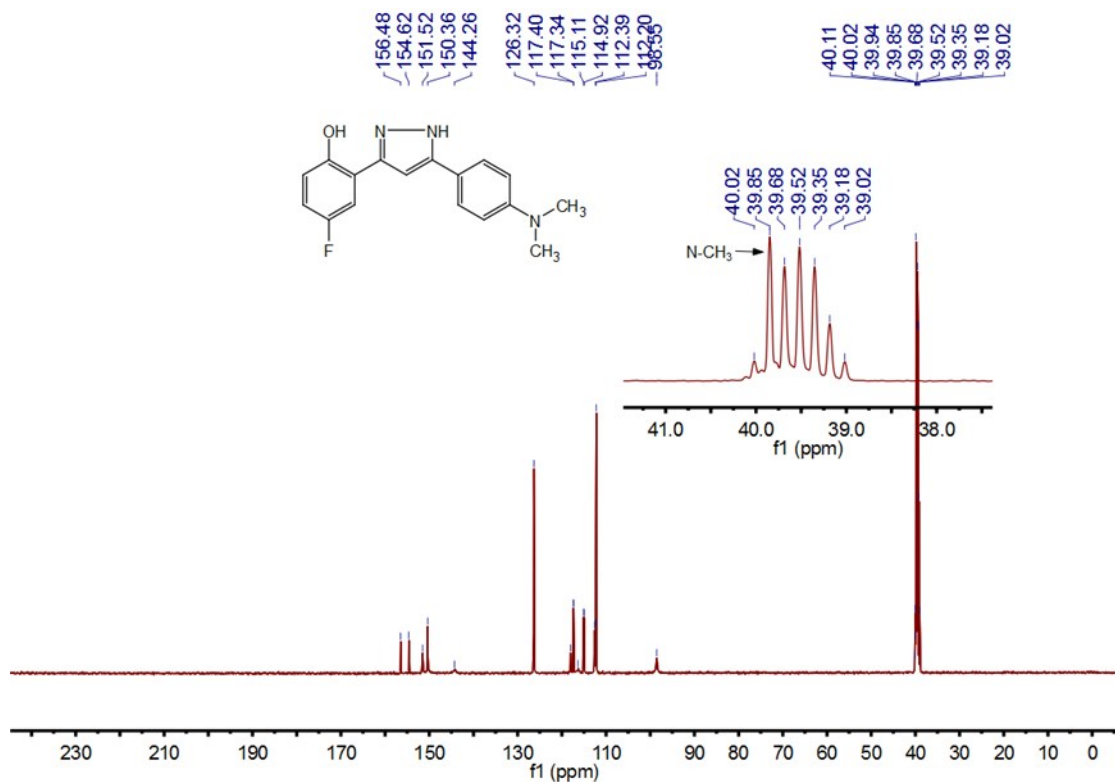


Figure S21. ^{13}C -NMR spectrum of compound **4** in $\text{DMSO}-d_6$ (125 MHz).

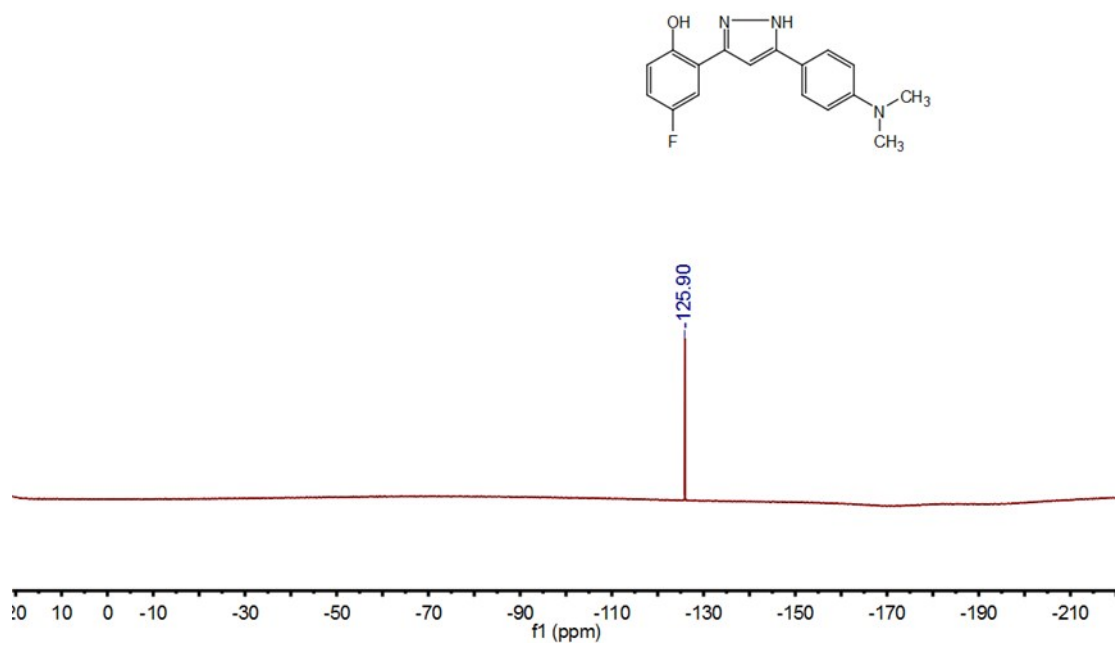


Figure S22. ^{19}F -NMR spectrum of compound 4 in CDCl_3 (470 MHz).

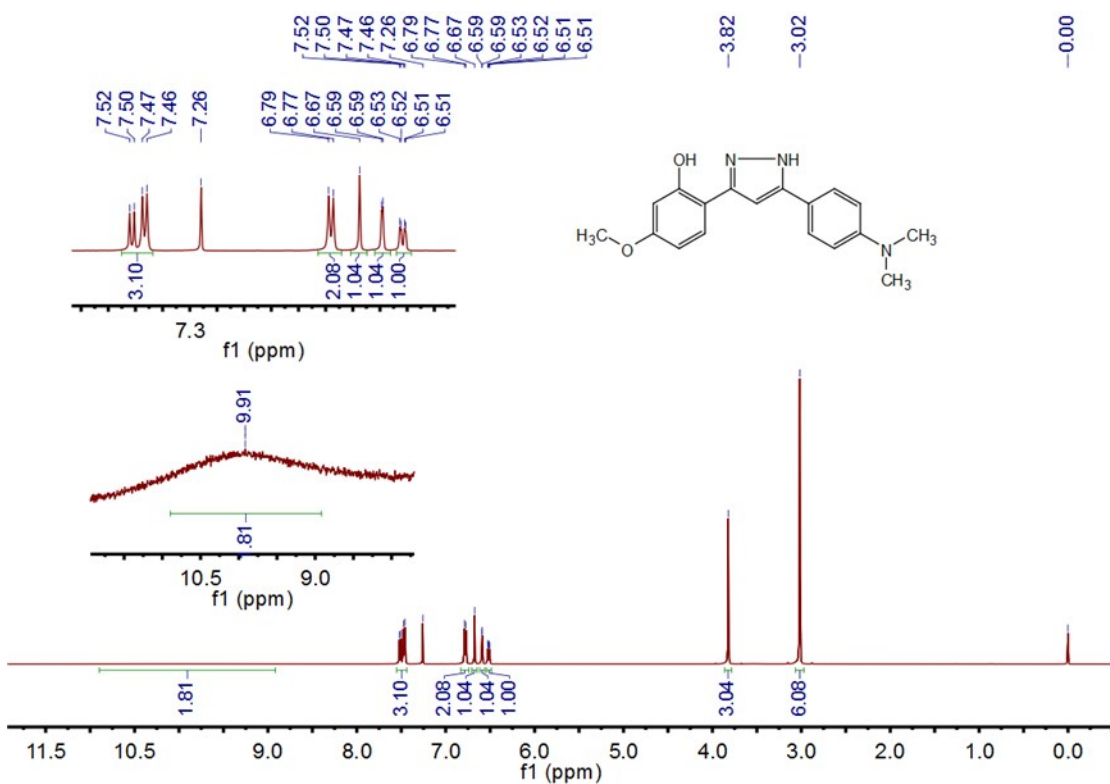


Figure S23. ^1H -NMR spectrum of compound **5** in CDCl_3 (500 MHz).

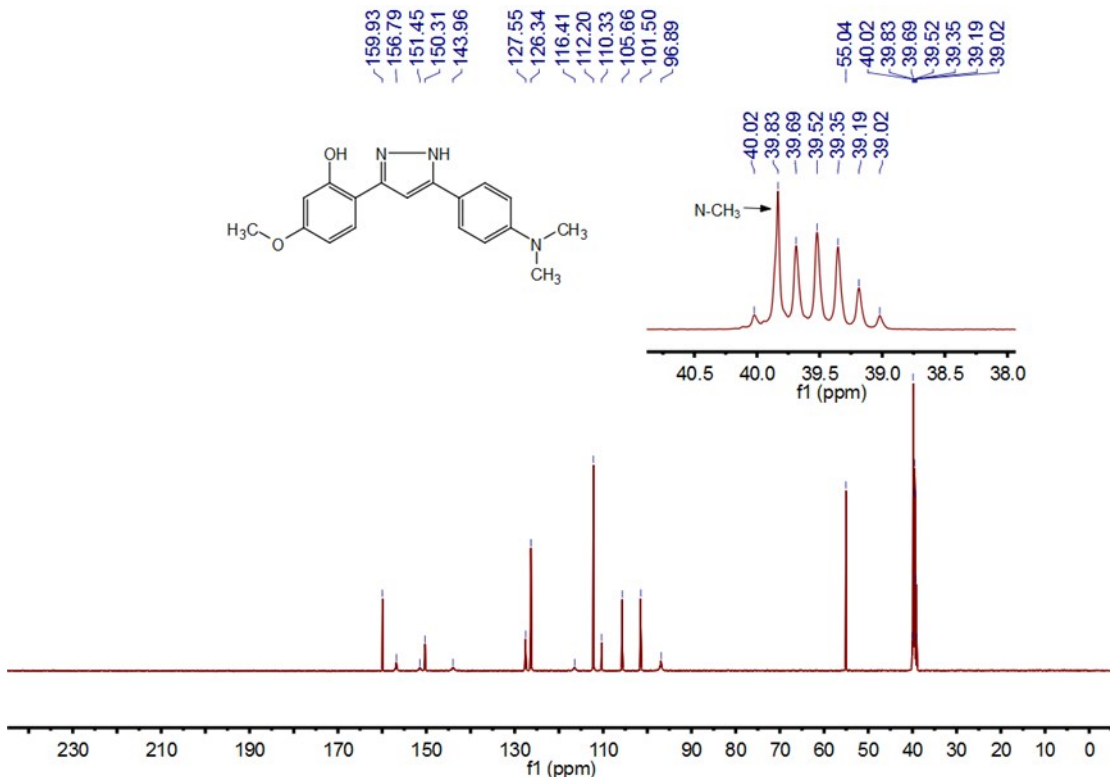


Figure S24. ^{13}C -NMR spectrum of compound **5** in $\text{DMSO}-d_6$ (125 MHz).

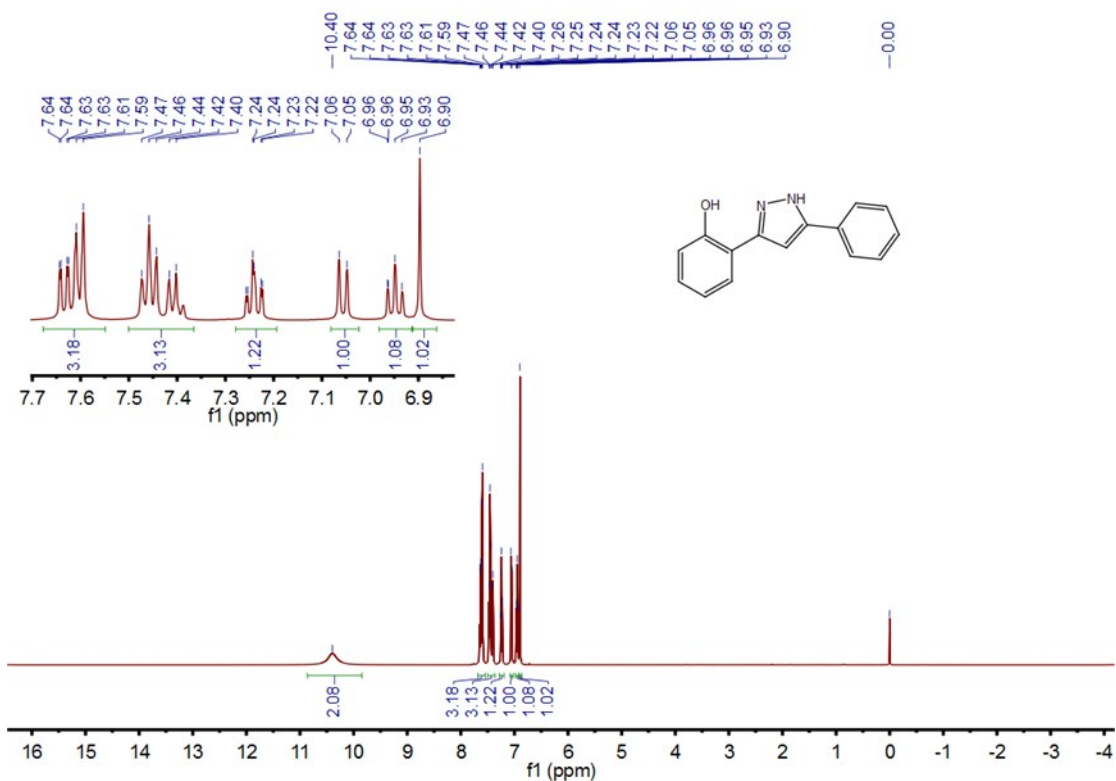


Figure S25. ^1H -NMR spectrum of compound **6** in CDCl_3 (500 MHz).

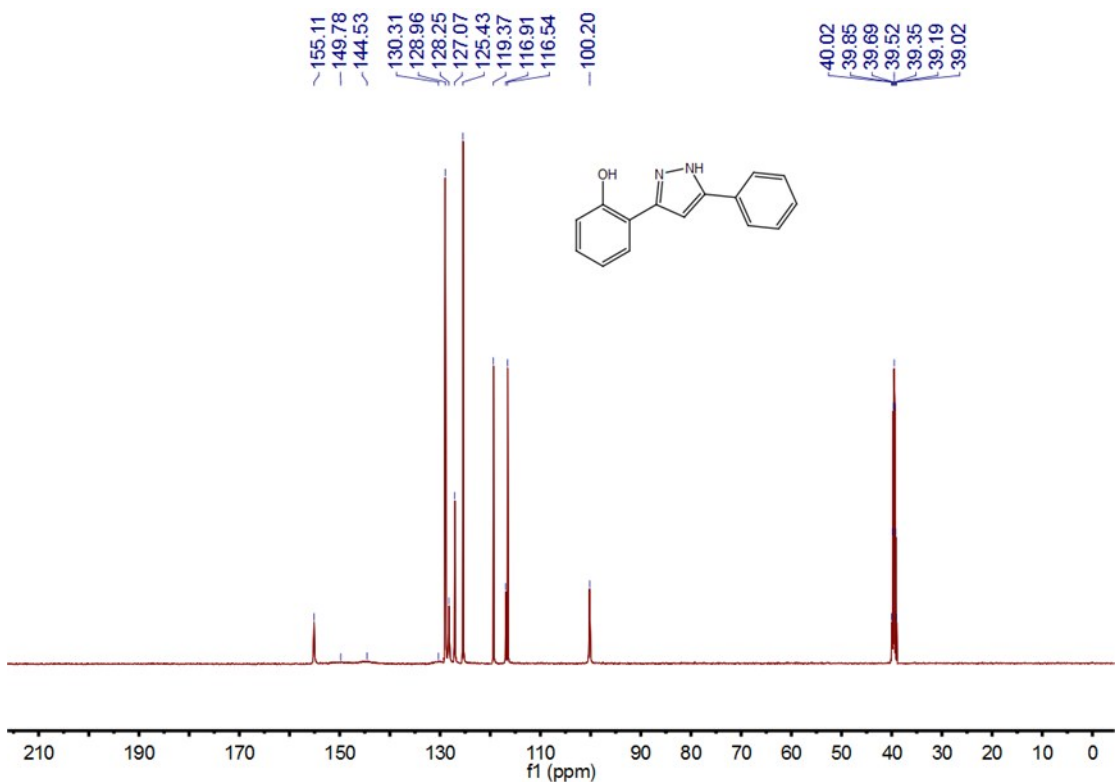


Figure S26. ^{13}C -NMR spectrum of compound **6** in $\text{DMSO}-d_6$ (125 MHz).

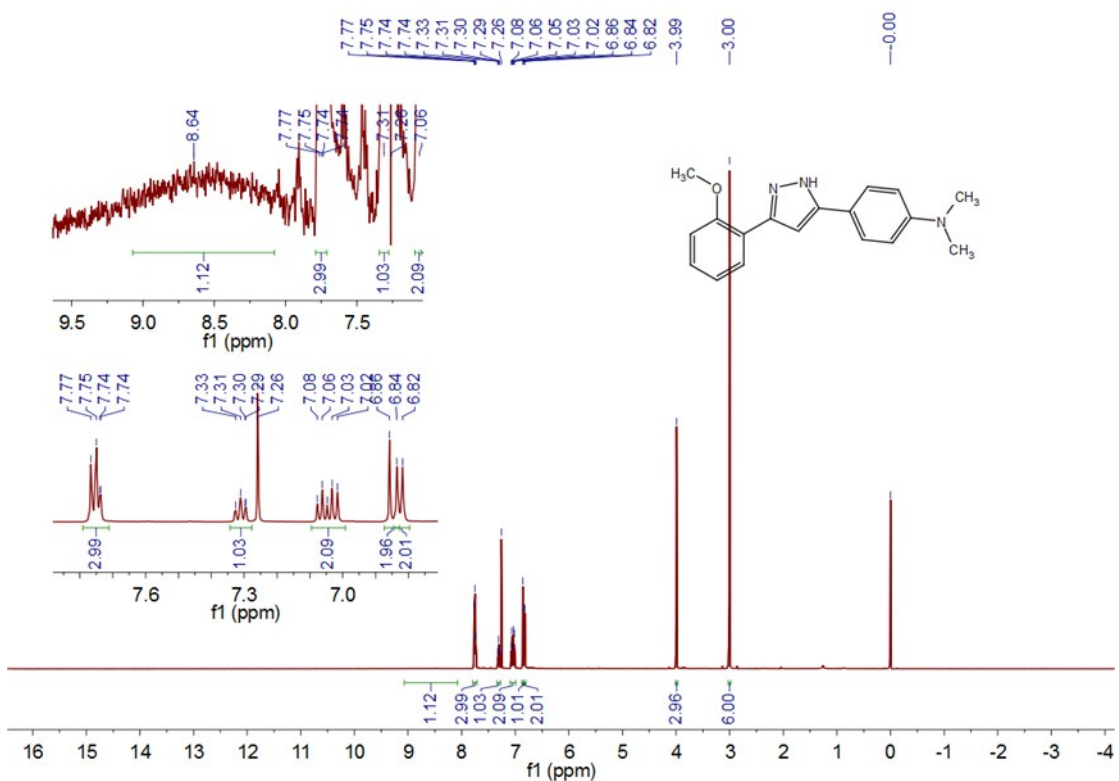


Figure S27. ^1H -NMR spectrum of compound 7 in CDCl_3 (500 MHz).

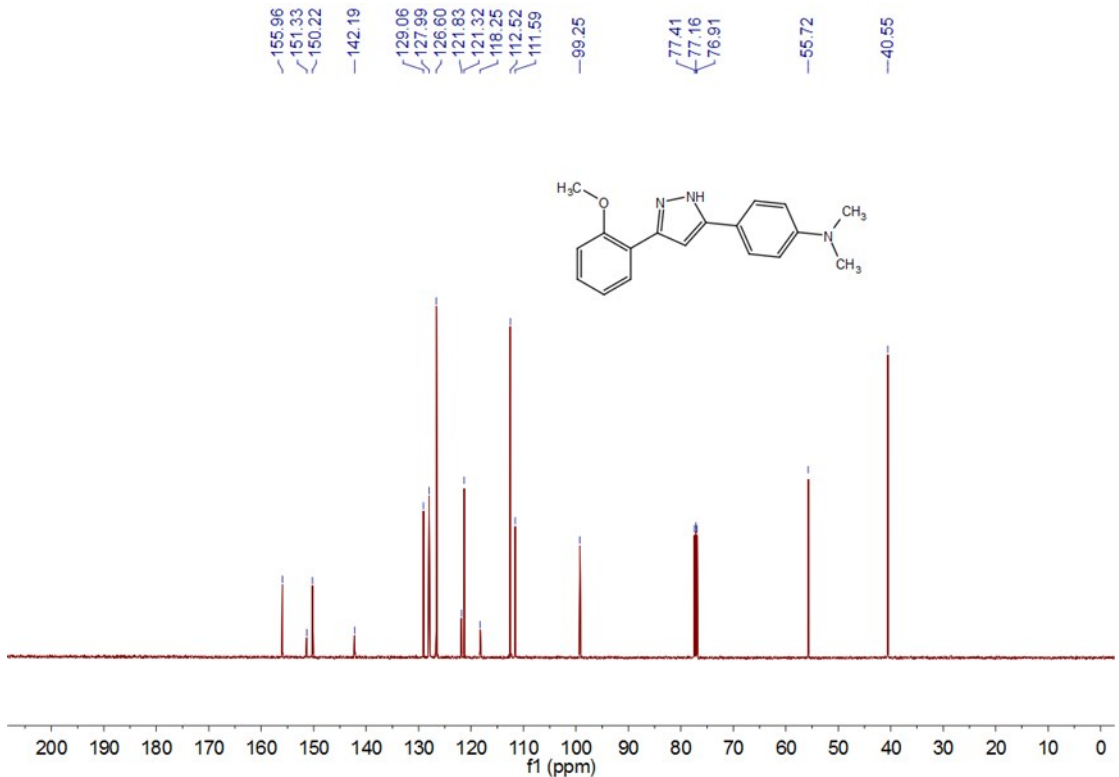


Figure S28. ^{13}C -NMR spectrum of compound 7 in CDCl_3 (125 MHz).